UMCG:

University of Groningen

Artistic edge and corner enhancing smoothing

Papari, Giuseppe; Petkov, Nicolai; Campisi, Patrizio

Artistic Edge and Corner Enhancing Smoothing

Giuseppe Papari, Nicolai Petkov, and Patrizio Campisi

Abstract—Two important visual properties of paintings and painting-like images are the absence of texture details and the increased sharpness of edges as compared to photographic images. Painting-like artistic effects can be achieved from photographic images by filters that smooth out texture details, while preserving or enhancing edges and corners. However, not all edge preserving smoothers are suitable for this purpose. We present a simple nonlinear local operator that generalizes both the well known Kuwahara filter and the more general class of filters known in the literature as "criterion and value filter structure." This class of operators suffers from intrinsic theoretical limitations which give rise to a dramatic instability in presence of noise, especially on shadowed areas. Such limitations are discussed in the paper and overcome by the proposed operator. A large variety of experimental results shows that the output of the proposed operator is visually similar to a painting. Comparisons with existing techniques on a large set of natural images highlight conditions on which traditional edge preserving smoothers fail, whereas our approach produces good results. In particular, unlike many other well established approaches, the proposed operator is robust to degradations of the input image such as blurring and noise contamination.

Index Terms—Adaptive filters, edge/corner enhancers, image region analysis, nonlinear filters, painterly image processing, smoothing methods.

I. INTRODUCTION

SMOOTHING is an important task in image processing [1]–[5]. The best known smoothing technique is low-pass linear filtering. The most widely used filter deploys a Gaussian kernel, since it has been proved to be very close to the optimality for noise rejection [6]. However, since linear low-pass filtering strongly attenuates high-frequency components, not only noise, but also edges and corners, are smoothed out. Therefore, there has been a remarkable effort to find a nonlinear operator able to remove texture and noise, while preserving edges and corners. In the following, we refer to such an operator as an edge and corner preserving smoother (ECPS).

Several ECPSs have been proposed in the literature [7]–[12]. The best known ones are based on median filtering [13], morphological analysis [14], [15], bilateral filtering [16], mean shift [17], total variation [18], and anisotropic diffusion [19]. The latter is probably the most popular ECPS, for which much research has been carried out in the last 15 years. However, it is not computationally efficient since it requires many iterations to achieve the desired output. A survey of ECPSs can be found in [20].

In the current work, we are interested in a specific aspect of ECPSs: their ability to produce images that are visually similar to paintings. Not all existing ECPSs are suitable for producing such an artistic effect. The class of ECPSs we consider here stems from the early work of Kuwahara [21], where a fast and conceptually simple ECPS is introduced. Specifically, in [21], a symmetric square neighborhood around each pixel of a gray level image is divided in four square subregions. The value of the central pixel is replaced by the gray level average over the most homogeneous subregion, i.e., the subregion with the lowest standard deviation. Although this operator was not designed for producing artistic images, the obtained effects are quite interesting.

The Kuwahara operator has been extended in several ways: by changing the shape of the subregions, from squares to pentagons, hexagons and, more recently, to circles [22], [23], by allowing overlapping subregions [24], [25], and by replacing the local averages with Gaussian weighted local averages [25]. In [23], a class of generalized Kuwahara filters, the value and criterion filter structure is introduced and efficient algorithms in terms of morphological filtering are provided. A formulation in terms of partial differential equations (PDEs) is given in [25]. However, all mentioned extensions suffer a common problem: the output of the operator is not uniquely determined when the minimum standard deviation is reached in more than one subregion. This problem is discussed in depth in this paper and it is shown that it may have dramatic effects in presence of noise.

In our contribution, we propose a new noniterative ECPS that generalizes the well known Kuwahara filter without suffering the related drawbacks. With respect to the proposed approach, our algorithm makes use of 1) a different set of weighting subregions for computing local averages and 2) a different combination criterion which generalizes the aforementioned minimum standard deviation rule and which does not suffer the above mentioned ill-posedness. The exposition is organized as follows: after a brief review of the Kuwahara filter and a discussion of its limitations in Section II, we introduce the proposed operator in Section III. We present and discuss experimental results in comparison with existing techniques in Section IV, and we draw conclusions in Section V.

G. Papari and N. Petkov are with the Institute of Mathematics and Computing Science, University of Groningen, 9700 AV Groningen, The Netherlands.

P. Campisi is with the Dipartimento Elettronica Applicata, Università degli Studi Roma Tre, Rome, Italy.
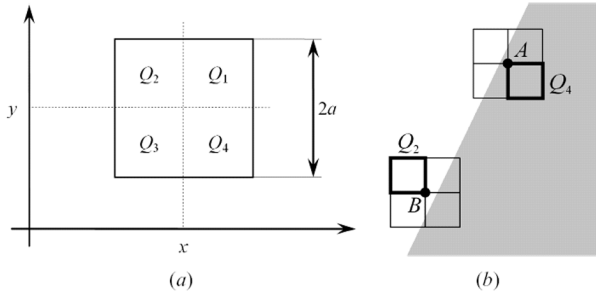
Fig. 1.   Kuwahara filtering: (a) subregions $Q_i, i = 1 \ldots 4$, on which local averages and standard deviations are computed. (b) The subregion with the smallest standard deviation (delineated by a thick line) determines the output of the filter.

II. Kuwahara Filter and Extensions

This section gives a short review of the Kuwahara filter, points out its theoretical and practical limitations, and presents an overview of its extensions proposed in the literature.

A. Review of the Kuwahara Filter

Let us consider a gray-level image $I(x,y)$ and a square of length $2a$ centered around a point (x,y) which is partitioned into four identical square subregions $Q_1, Q_2, Q_3,$ and Q_4 [Fig. 1(a)]

$$
\begin{cases}
Q_1(x,y) = [x, x+a] \times [x, y+a] \\
Q_2(x,y) = [x-a, x] \times [y, y+a] \\
Q_3(x,y) = [x-a, x] \times [y-a, y] \\
Q_4(x,y) = [x, x+a] \times [y-a, y]
\end{cases}
\tag{1}
$$

where the symbol "$\times$" denotes the Cartesian product.

Let $m_i(x,y)$ and $s_i(x,y)$ be the local average and the local standard deviation, respectively, computed on each subregion $Q_i(x,y), i = 1 \ldots 4$. For a given point (x,y), the output $\Phi(x,y)$ of the Kuwahara filter is defined as the local average value $m_i(x,y)$ that corresponds to the ith subregion providing the minimum local standard deviation value $s_i(x,y)$ [21]. This can be formulated as follows:

$$
\Phi(x,y) = \sum_i m_i(x,y) f_i(x,y)
\tag{2}
$$

where

$$
f_i(x,y) = \begin{cases}
1, & s_i(x,y) = \min_k \{ s_k(x,y) \} \\
0, & \text{otherwise.}
\end{cases}
\tag{3}
$$

Fig. 1(b) shows the behavior of the Kuwahara operator in the proximity of an edge. When the central point (x,y) is on the dark side of the edge (point A), the output is equal to m_4, which is the local average computed on the subregion that completely lies on the dark side (Q_4 in our case). It is the most homogeneous area, having the smallest local standard deviation s_i among the four subregions. On the other hand, as soon as the point (x,y) moves to the bright side (point B), the output is determined by another subregion that lies completely in the bright area (Q_2 in our case), since now that subregion has the minimum standard
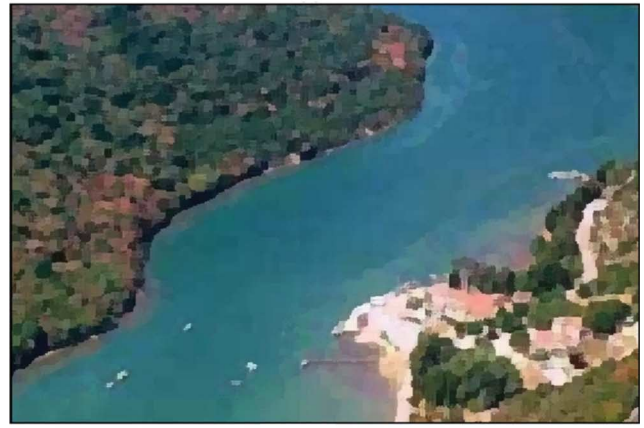
Fig. 2.   (a) Test image (480×320 pixels) and (b) the output of the Kuwahara filter. The block structure due to the Gibbs phenomenon is well visible on the output of the Kuwahara filter, especially on strongly textured areas.

deviation s_i. This flipping mechanism guarantees the preservation of edges and corners, while the local averaging smooths out texture and noise.

B. Limitations of the Kuwahara Filter

One limitation of the Kuwahara filter is the block structure of the output, particularly evident on textured areas (Fig. 2), that is due to the square shape of the regions Q_1 through Q_4 and to the Gibbs phenomenon [26]. This problem can be avoided by using different shapes for the subregions Q_i and by replacing the local averages with weighted local averages. We will discuss this in more detail in Section II-C.

A more serious problem is that the Kuwahara filter is not a mathematically well defined operator: every time the minimum value of s_i is reached by two or more subregions, the output of the Kuwahara operator cannot be uniquely determined, because it is unclear which subregion should be chosen. As we will illustrate with a simple 1-D example, two subregions with equal standard deviations $s_1 = s_2$ can have considerably different local average values m_1 and m_2.

For 1-D signals, the Kuwahara filter is defined as follows: two local averages $m_1(x)$ and $m_2(x)$, and two local standard
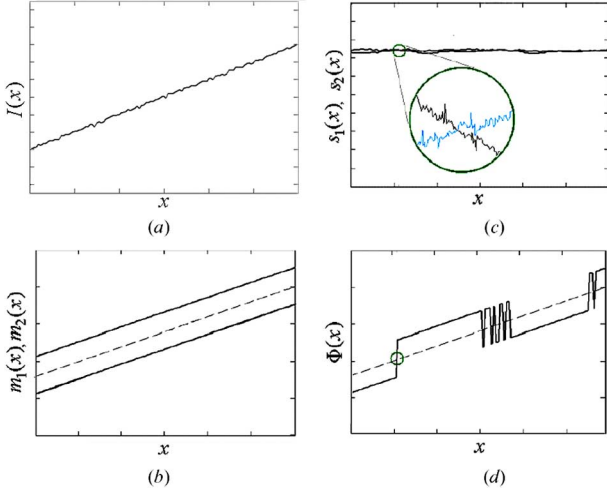
Fig. 3. Effect of the indetermination of the Kuwahara operator for a 1-D signal. (a) Input signal $I(x) = x$ corrupted by very small additive noise, (b) the two local averages $m_i(x)$, and $m_2(x)$, (c) the two local standard deviations $s_1(x)$ and $s_2(x)$, and (d) the output of the Kuwahara filter. The standard deviations are almost equal and the transitions from $m_1(x)$ to $m_2(x)$ and vice versa in the output occur randomly at the zero crossings of $s_1(x) - s_2(x)$.
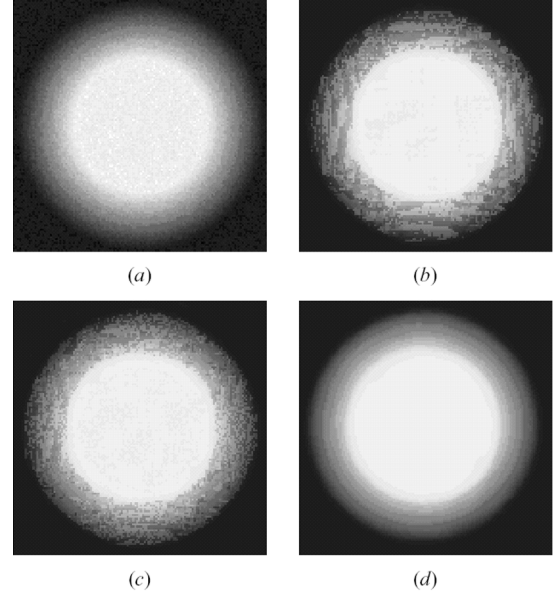

Fig. 4. Effect of the indetermination of the Kuwahara filter for a 2-D signal. (a) Input image. Output of the Kuwahara filter (b) without and (c) with the additional criterion (4), and (d) output of the operator proposed in this paper. Unperceivable additive noise in the input image has a strong effect on the output of the Kuwahara filter and its modification according to the additional criterion (4) brings only a small improvement. The approach proposed here is much more stable in this respect.

deviations $s_1(x)$ and $s_2(x)$ are computed on the two intervals $[x - a, x]$ and $[x, x + a]$, respectively, around each point x. The output at x is given by the value $m_1(x)$ or $m_2(x)$, which corresponds to the smaller one of $s_1(x)$ and $s_2(x)$. It is straightforward to see that if we consider the input signal $I(x) = x$, the two local averages $m_1(x)$ and $m_2(x)$ are different, with $m_2(x) - m_1(x) = a$, while the two standard deviations are equal, $s_1(x) = s_2(x) = \sqrt{a^3/(12)}$. Therefore, for such an input signal, the output of the Kuwahara operator is not uniquely determined. However, in real applications where noise is always present it is very unlikely that the estimated standard deviations have the same value; therefore, the algorithm will randomly choose either $m_1(x)$ or $m_2(x)$ depending on the noise. This instability of the output of the Kuwahara operator is illustrated in Fig. 3.

Commonly, there are two ways to try to solve this problem [23]: the first solution is to set the output $\Phi(x)$ equal to $[m_1(x) + m_2(x)]/(2)$ for those values of x for which the difference $|s_2(x) - s_1(x)|$ is below a given threshold T. This method is robust to noise but, as pointed out in [23], edges are not very well preserved. Alternatively, if $|s_2(x) - s_1(x)| < T$, $\Phi(x)$ can be set to the value of $m_i(x)$ that is closer to $I(x)$

$$\Phi(x) = m_k(x), \quad k = \arg\min_i |m_i(x) - I(x)|. \quad (4)$$

This latter method results in a better edge enhancement, but it is more sensitive to noise. Moreover, the indetermination discussed above would still persist for the input signal $I(x) = x$, since $m_1(x)$ and $m_2(x)$ are equally close to $I(x)$.

Fig. 4 shows the effect of such a problem for a 2-D input signal consisting of a blurred circle corrupted by a very low-power Gaussian noise [Fig. 4(a)]. Though the noise in the test image has a very low level, it has a considerable effect on the

output of the Kuwahara filter [Fig. 4(b)]. On the shadowing corona around the circle, the four values $s_i, i = 1 \ldots 4$ are almost equal to each other and their differences are due only to the noise. Therefore, we obtain an output which varies randomly as the selection jumps from one subregion Q_i to another, thus producing the instabilities shown in Fig. 4(b). Fig. 4(c) shows the small improvement brought by the additional criterion (4), but the filtered image is still noisier than the input. For comparison, Fig. 4(d) shows the result obtained with the operator that we will introduce in Section III.

C. Generalizations of the Kuwahara Filter

Over the last two decades, several extensions of the Kuwahara operator have been proposed by changing the number and the shape of the subregions and by replacing local averages with weighted local averages. In [22], the square subregions Q_i are replaced by pentagons and hexagons. More recently, in [24], circular subregions are considered, and, in [23] and [25], a larger set of overlapping subregions is taken into account. In [25], the local averages are replaced by Gaussian weighted local averages in order to avoid the Gibbs phenomenon [26] (Gaussian Kuwahara filtering). All these extensions can be unified in the following general framework: N weighted local averages m_i and standard deviations $s_i, i = 1 \ldots N$ are defined by the following convolutions of the input image I with weighting functions w_i

$$m_i = I * w_i$$
$$s_i^2 = I^2 * w_i - m_i^2, \quad \iint_{\mathbb{R}^2} w_i(x, y) \mathrm{d}x \mathrm{d}y = 1. \quad (5)$$

The Kuwahara filter is a special case of this class of filters, with $w_i(x,y) = 1$ if $(x,y) \in Q_i$, and $w_i(x,y) = 0$; otherwise, $i = 1 \dots 4$.

For each point (x,y), the output $\Phi(x,y)$ is obtained by the *minimum standard deviation criterion* (MSDC) expressed by (2) and (3). Therefore, all these methods suffer the indetermination problem discussed in Section II-B.

A computationally appealing algorithm is obtained from (5), when all the weighting functions w_i are translated versions of a given function w. In this case, the filter can be implemented by using only two convolution operations, independently of the number of subregions N [23]. For this reason, all the possible translated versions of the function w in a given neighborhood of the central pixels are considered in [23] and [25]. This class of filters is called value and criterion filter structure (VCFS). When the weighting function w is Gaussian one gets the so called Gaussian Kuwahara filter [25].

III. PROPOSED OPERATOR

The approach we propose is a generalization of the VCFS. The main contribution of the present study is a new combination criterion that does not suffer the limitations of the MSDC, and the use of different weighting functions w_i which are more suitable for preserving corners and edges. In this section, we first introduce the proposed operator for gray level images, and then we present a straightforward extension to color images.

A. Gray Level Images

We divide a circular region around each pixel in N equal sectors $S_i, i = 1 \dots N$, over which we compute weighted local averages and local standard deviations. Let $g_\sigma(x,y)$ be the following 2-D Gaussian kernel:

$$g_\sigma(x,y) = \frac{1}{2\pi\sigma^2} e^{-\frac{x^2+y^2}{2\sigma^2}}. \tag{6}$$

The sectors S_i are defined by the following cutting functions $V_i(r,\vartheta)$, expressed in polar coordinates:

$$V_i = U_i * g_{\sigma/4},$$
$$U_i(r,\vartheta) = \begin{cases} N, & i - \frac{1}{2} < \frac{N}{2\pi}\vartheta < i + \frac{1}{2} \\ 0, & \text{otherwise.} \end{cases} \tag{7}$$

The weighting functions w_i are defined as products between the Gaussian mask g_σ and the cutting functions V_i

$$w_i = g_\sigma \cdot V_i. \tag{8}$$

Fig. 5 shows the weighting functions (8) for the case $N = 8$ sectors. Note that

$$\frac{1}{N}\sum_{i=1}^{N} V_i(x,y) = 1, \quad \frac{1}{N}\sum_{i=1}^{N} w_i(x,y) = g_\sigma(x,y). \tag{9}$$
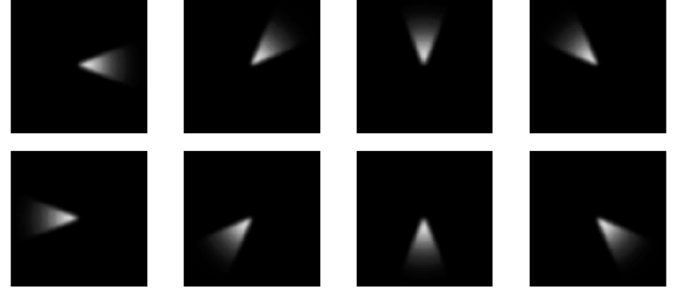
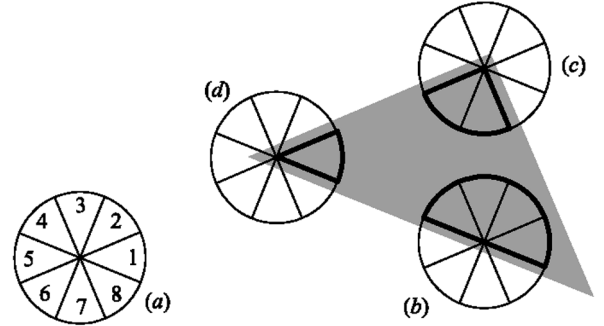Fig. 5. Eight weighting functions w_i used in the proposed operator.

Fig. 6. Sector selection in various situations: (a) homogeneous (texture) area, (b) edge, (c) corner, and (d) sharp corner. The sectors selected to determine the output are delineated by a thick line.

Once m_i and s_i are computed according to (5), the mathematical expression of the proposed combination criterion is still the linear combination (2) where the discontinuous functions $f_i(x,y)$ (3) are replaced by the following functions:

$$f_1^{(q)}(x,y) = \frac{s_i^{-q}(x,y)}{\sum_i s_i^{-q}(x,y)} \tag{10}$$

where q is a parameter. Thus, the output $\Phi_q(x,y)$ is given by

$$\Phi_q = \frac{\sum_i m_i s_i^{-q}}{\sum_i s_i^{-q}} \tag{11}$$

where the explicit dependence on (x,y) has been omitted for simplicity of notation. According to (11) the filter output $\Phi_q(x,y)$ is a weighted average of the local averages $m_i(x,y)$, with weights equal to $s_i^{-q}(x,y)$. For positive values of q, more importance is given to the values of m_i that correspond to smaller values of s_i.

For $q = 0$, $\Phi_q(x,y)$ reduces to the arithmetic mean of $m_i(i = 1 \dots N)$. Taking into account (9), for $q = 0$, the proposed operator is equivalent to a linear Gaussian filter. On the opposite extreme, for $q \to \infty$ the functions $f_i^{(q)}(x,y)$ of (10) reduce to the functions $f_i(x,y)$ of (3), thus obtaining MSDC.

For finite positive values of q, the proposed operator is an intermediate case between a Gaussian and a value and criterion
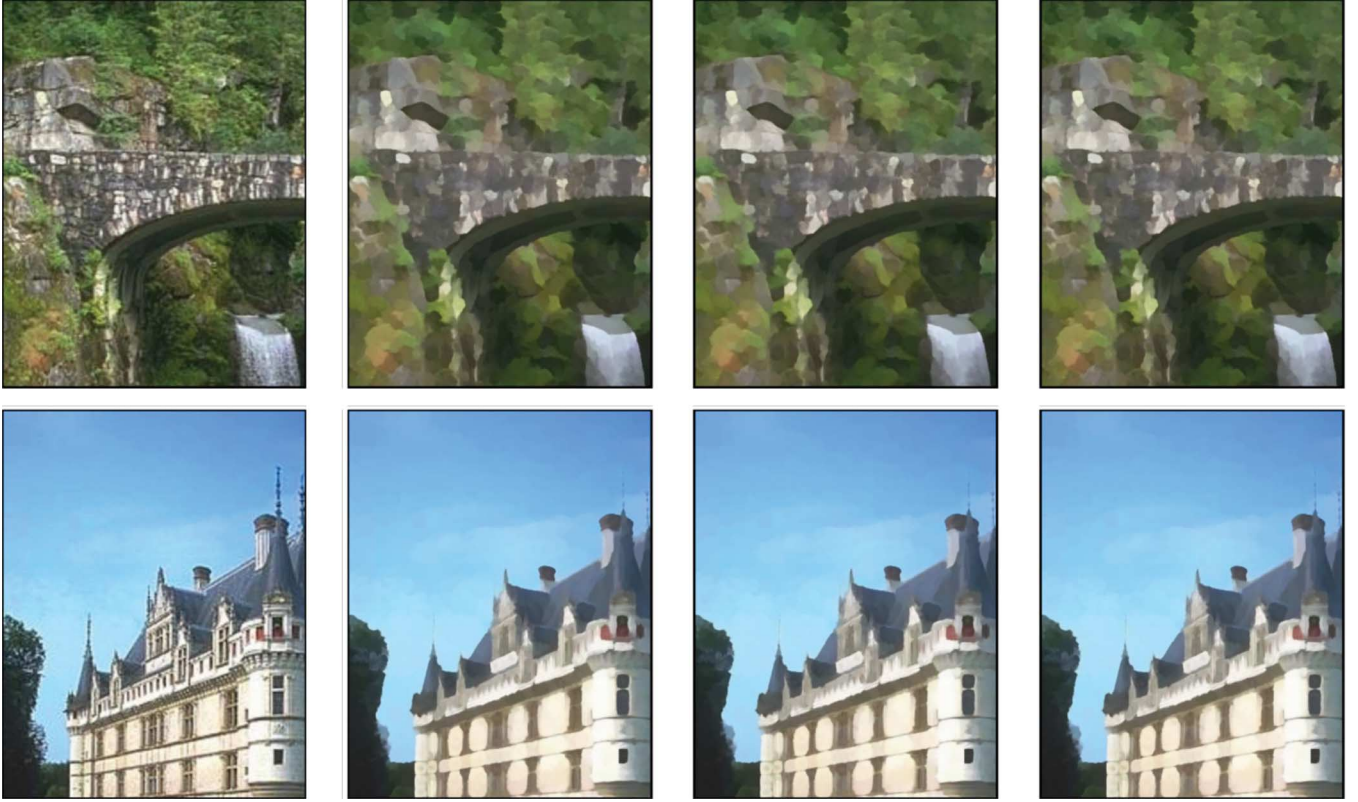
Fig. 7. Effect of the different choices of the space color on the smoothing process. From left to right: input images (375×480 pixels) and outputs of the proposed operator for the color spaces RGB, $\mathrm{YC_bC_r}$, $\mathrm{L^*a^*b^*}$. The differences between the different outputs are minimal.

filter, since it behaves like a Gaussian filter in homogeneous and textured regions, and like a value and criterion filter around contours and corners of objects. Thus, since Gaussian filtering is more suitable for noise rejection and value and criterion filtering is more suitable for preserving edges, we get the advantages of both. The parameter q controls the sharpness of the transition between the linear Gaussian-like behavior and the VCFS-like behavior. This is illustrated in Fig. 6. On areas that contain no edges (case a), the values $s_i, i = 1 \ldots N$, are very similar to each other; therefore, the output Φ_q is close to the average of the m_i values. The operator behaves very similarly to a Gaussian filter, thus texture and noise are averaged out and the Gibbs phenomenon is avoided. On the other hand, in the presence of an edge (case b), the sectors that cross it give higher s_i values than the other sectors. If q is sufficiently large (for instance, $q \geqslant 4$), the sectors intersected by the edge $(S_5 - S_8)$ give a negligible contribution to the value of Φ_q. Similarly, in presence of corners (case c) and sharp corners (case d), only those sectors which fall inside the corner $(S_6, S_7$ for case c and S_1 for case $d)$ give an appreciable contribution to the value of Φ_q, whereas the other sectors have a negligible effect.

The choice of using circular sector shaped regions R_i for computing the local averages is particularly suitable for preserving edges and sharp corners. The combination rule expressed by (11) allows us to, for each pixel, *automatically select* the sectors which provide the best coverage of either the edge or the corner under analysis. Finally, we point out that our combination criterion does not suffer the indetermination of the

Kuwahara operator, since no hard selections are involved. Only theoretically, the righthand side of (11) would be undefined if some s_i is equal to zero, but the indetermination can easily be removed by using the well known De l'Hospital rule. Moreover, since the regions on which the weighting functions w_i are not zero slightly overlap, the case $s_i = 0$ can occur only in regions where the input signal $I(x, y)$ is constant.

B. Color Images

The generalization of the discussed method for color images is straightforward: let $I^{(1)}(x, y)$, $I^{(2)}(x, y)$, $I^{(3)}(x, y)$ be the color components in a given color space. The local averages $m_i^{(c)}(x, y)$ and the local standard deviations, $s_i^{(c)}(x, y), c = 1, 2, 3, i = 1, \ldots, N$, are computed according to (5) for each component $I^{(c)}(x, y)$. Afterward, the output Φ_q is computed similarly to (11) as follows:

$$\Phi_q = \frac{\sum_i \mathbf{m}_i s_i^{-q}}{\sum_i s_i^{-q}} \tag{12}$$

with

$$\mathbf{m}_i = \left[m_i^{(1)}, m_i^{(2)}, m_i^{(3)} \right]^T, \quad s_i = \sqrt{\sum_{c=1}^{3} \left[s_i^{(c)} \right]^2}. \tag{13}$$

Fig. 8.   (a)–(b) Output of the proposed operator for the test image shown in Fig. 2(a), with (a) $\sigma = 1.5$, (b) $\sigma = 3$. Results of (c) morphological structural closing [14], (d) morphological area open-closing, (e) median [13], and (f) bilateral filtering [16].

Note that this is not equivalent to apply the operator to each color component independently, since the coefficients $s_i^{-q}/\sum_i s_i^{-q}$ are the same for all three color components. If the three components was treated separately, the coefficients would be different for each color component and spurious colors would be introduced on borders of areas with very different chrominance. An analogous effective strategy for avoiding color artifacts has been proposed in [16].

Equation (12) can be applied to any color space. We found that the choice of a color space does not significantly affect the final result. In fact, from (11), we see that the operator output Φ_q is determined by 1) the color averages $\mathbf{m}_i$ and 2) the standard deviations $s_i, i = 1 \ldots N$. The colors $\mathbf{m}_i$ are independent on the color representation only if the transformation rules between different color spaces are linear. However, for sufficiently homogeneous regions, these differences are not very pronounced also for nonlinear color transformations. Since, in (12), the major contribution is given by the most homogeneous regions, we conclude that the color averages $\mathbf{m}_i$ are not significantly influenced by a specific choice of a color space, un-
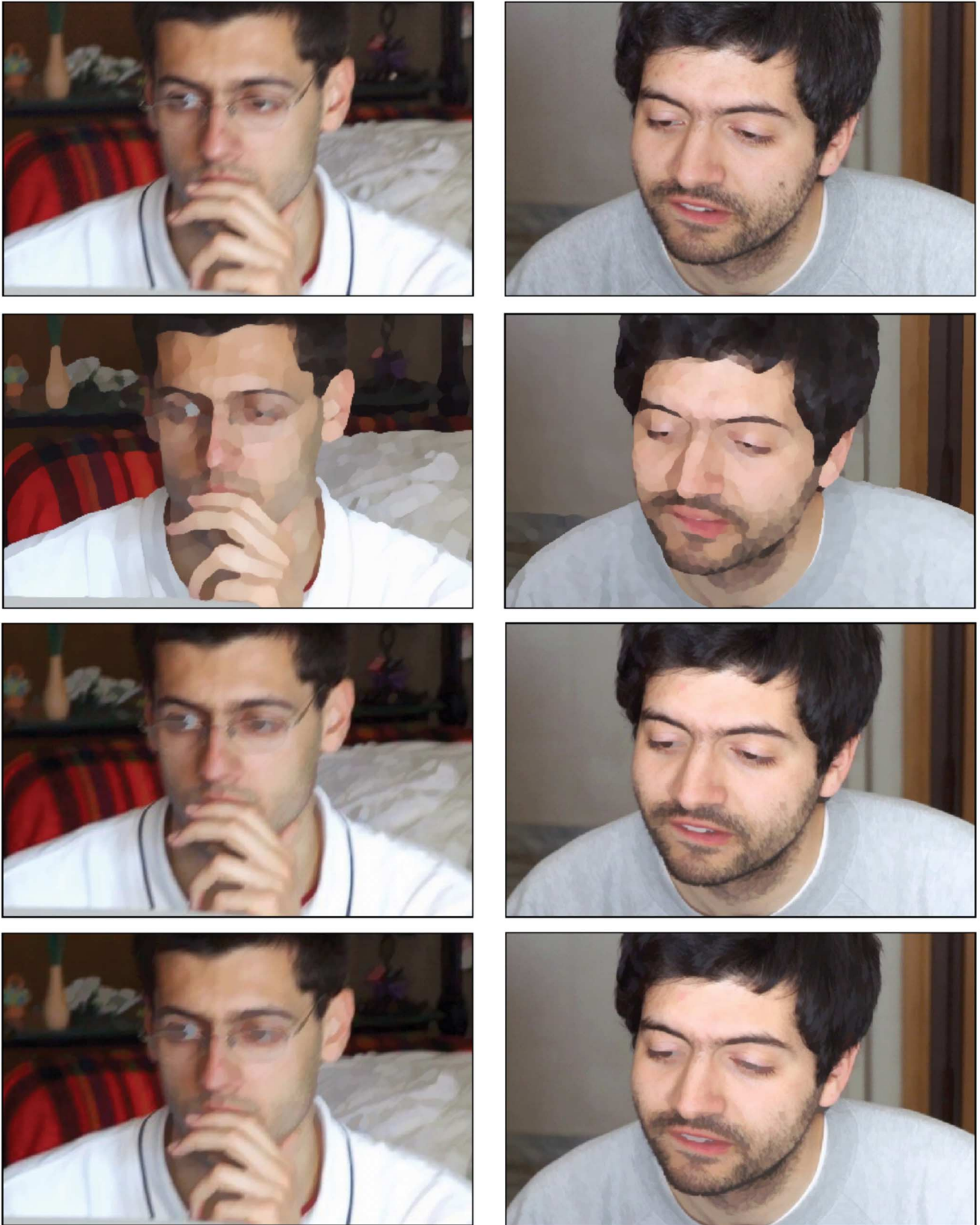
Fig. 9. Comparison of the proposed operator with morphological area open-closing [15] First row: input images (555 × 347 pixels); second row: output of the proposed operator; third and fourth row: output of area opening with $A_{min} = 50$ and $A_{min} = 100$. In these examples, area opening does not produce artistic effects.

lessimages with very low signal to noise ratio are taken into account.

Formally, the standard deviations s_i depend on the color space choice, as well. However, for natural images, it is

Fig. 10. Example of the effect of the indetermination of the Kuwahara filter on natural images: (a) Test image (160 × 270 pixels), and the outputs of (b) the Kuwahara, (c) the Gaussian Kuwahara, and (d) the proposed filter. The arrows point at some of the discontinuities introduced by the Kuwahara-like operators. Such discontinuities are not present with the proposed approach.

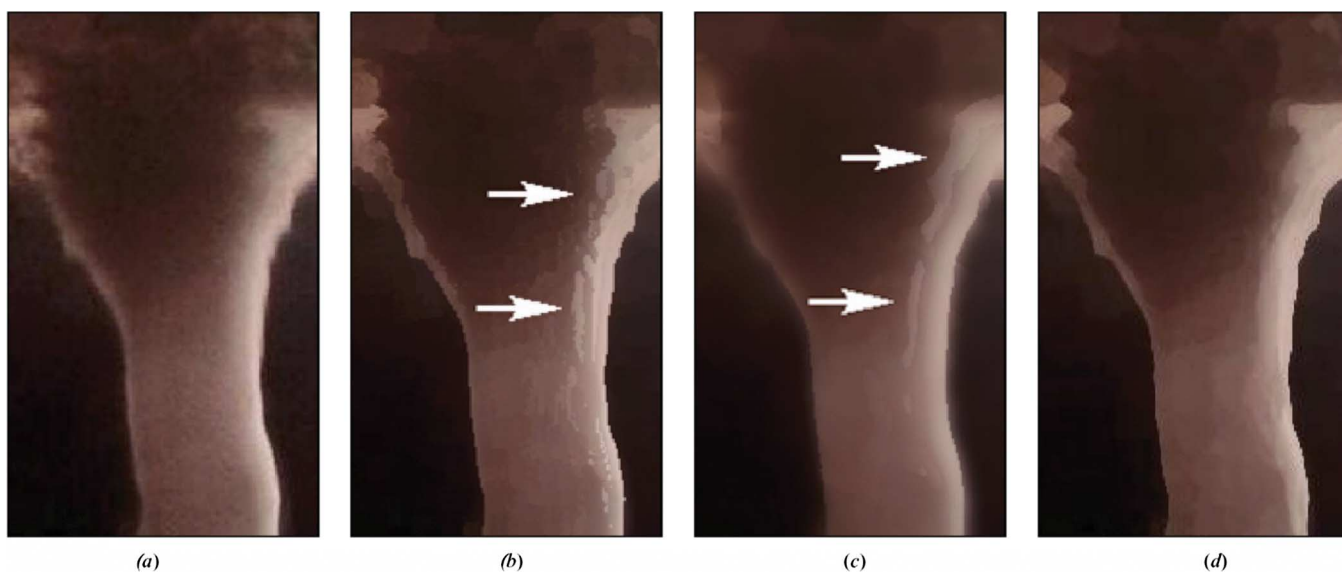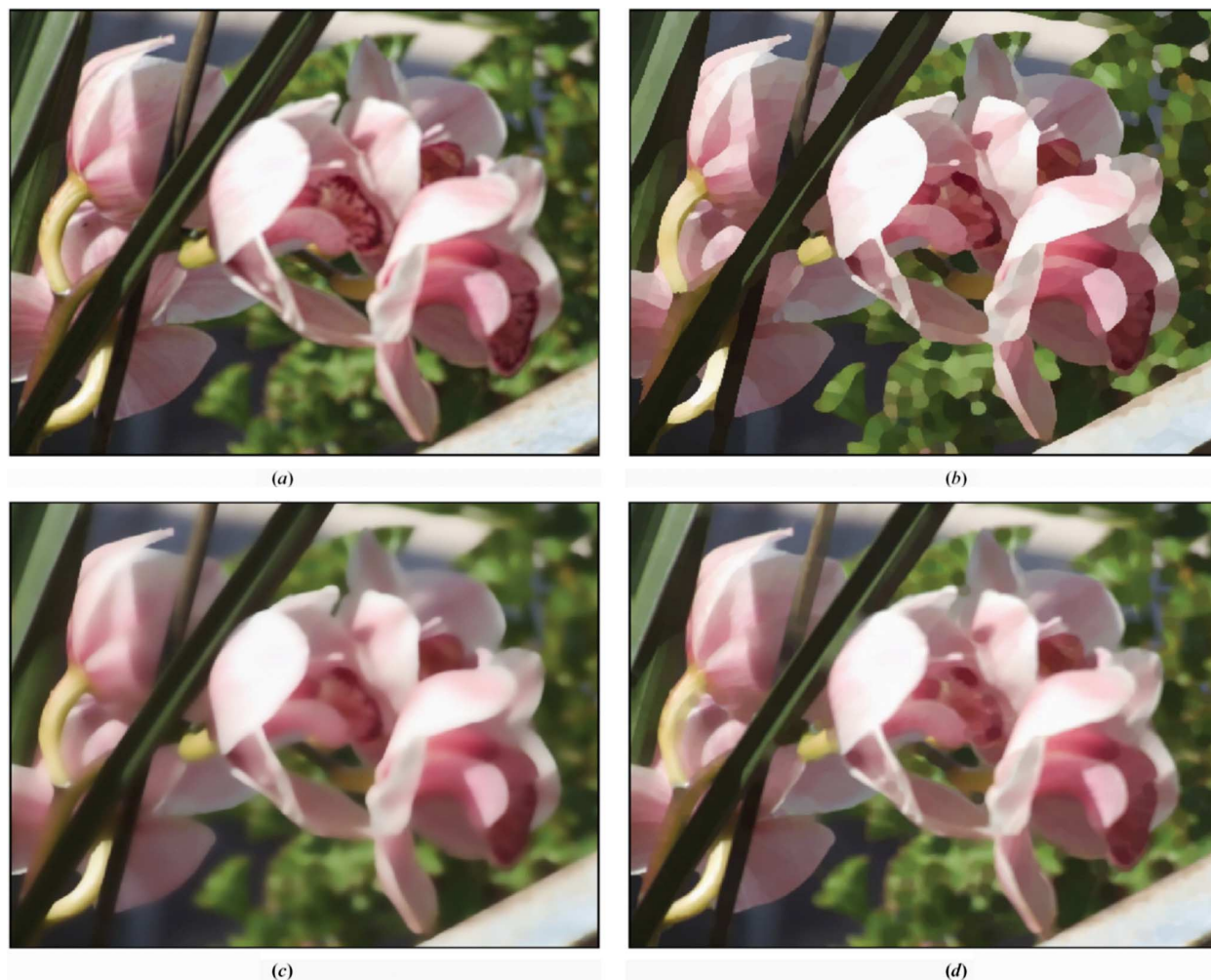

Fig. 11. Comparison of different methods for an image that contains blurred regions: (a) test image (508 × 409 pixels), and outputs of (b) the proposed operator, (c) bilateral [16] operator, and (d) median [13] filter. The proposed method succeeds in restoring the blurred edges, while the other two fail.

very unlikely that the region homogeneity is affected by the employed color space used to represent the image. Therefore, in (12), a higher weight is given to more homogenous regions independently of the deployed color space. Fig. 7 illustrates that the choice of the color space does not affect substantially the results.

IV. EXPERIMENTAL RESULTS

In this section, we present some experimental results illustrating the ability of the proposed operator to generate artistic images. Specifically, in Section IV-A, we compare it with other existing ECPS algorithms. The influence of the parameters σ, q and N is discussed in Section IV-B.

A. Comparison With Existing Approaches

We compare the proposed approach with Kuwahara [21], Gaussian Kuwahara [25], median [13], bilateral [16], and morphological [14], [15] filters, which are the most common ECPSs encountered in the literature. As for the Gaussian Kuwahara filtering, in our work we have implemented a simplified version, by using only four translated Gaussian kernels, centered on the points $(\pm\sigma, \pm\sigma)$.

The images presented here, Figs. 8–14, are rendered at reduced resolution. Full size images, together with a larger set of examples, are available under an URL.[1] Unless differently stated, we use the parameter values according to Table I.

Fig. 8(a) and (b) shows the outputs of our operator for the test image shown in Fig. 2(a) for two different values of the smoothing parameter $\sigma(\sigma = 1.5, \sigma = 3)$ defined in (6). By comparing them with Fig. 2(b), we can see the improvement achieved by our operator with respect to the Kuwahara filter: the blocking effect due to the Gibbs phenomenon is no longer present. The overall effect of the proposed operator is more similar to a painting than the effect obtained by the application of the Kuwahara filter [Fig. 2(b)].

Fig. 8(c) shows the output of a structural morphological closing with a disk as a structuring element. Morphological filtering is able to smooth out texture and noise while preserving edges and corners, but the filtered image presents many undesired spots, having the shape and size of the structuring element. Morphological area open-closing [15] does not introduce spots and in some cases it can produce nice painting-like images [Fig. 8(d)]. However, in several other cases, its output does not substantially differ from the input image, as illustrated by Fig. 9. Moreover, due to its flattening property, area open-closing may produce effects that are visually similar to a nonlinear distortion of the input image (see, for instance, the change in the brightness of the forehead of the man in Fig. 9, third and fourth row, second column with respect to the input image).

Fig. 8(e) and (f) shows the output of bilateral and median filtering, respectively. Although these techniques have very good performance in smoothing texture while preserving edges and corners, from a perceptual point of view, the obtained result is more similar to texture blurring or defocusing rather than to a painting.

In Fig. 10, we see the effect of the VCFS ill-posedness on a real image that presents slow and gradual luminance changes in presence of noise [Fig. 10(a), on the right side of the hurricane]. In the presence of shadowing, the Kuwahara operator introduces spurious discontinuities [marked by arrows in Fig. 10(b)]. These

[1]http://www.cs.rug.nl/~imaging/artisticsmoothing

discontinuities are reduced but not completely eliminated by the Gaussian Kuwahara filter [see the arrows in Fig. 10(c)]. However, edge preservation is worse, as we can see, for instance, on the right side of the hurricane. In contrast, our operator smoothes out texture and noise, and enhances edges without introducing spurious discontinuities.

Besides preserving edges, the proposed operator sharpens edges that are blurred in the original image. We can observe this effect, for instance, by comparing the right side contour of the hurricane in Fig. 10(a) and (d). This property has a noticeable contribution to achieving a painting-like effect. It is worth pointing out that, in general, preserving shadowed areas is the hardest task for operators aimed to sharpen blurred edges, since spurious discontinuities tend to be introduced. In this respect, our operator performs well as illustrated by Fig. 10(d).

The aforementioned edge enhancing property makes our operator robust when acting on blurred images as depicted in Fig. 11, where it is shown how the proposed operator performs in comparison with other well established edge preserving smoothers, like the bilateral [Fig. 11(c)] and the median filters [Fig. 11(d)]. Specifically, bilateral and median filtering can preserve an edge that is already sharp in the original image but they are not able to sharpen blurred edges.

The robustness of our operator to blurring can be exploited in order to obtain large high-quality pictures with a painting-like effect when small input images are used, as shown in Fig. 12. The test image (221×150 pixels) shown in Fig. 12(a) has been upsampled by a factor of 2 using a standard technique, thus obtaining the blurred image shown in Fig. 12(b).

The output of the proposed operator, shown in Fig. 12(c), is a sharp-edged high-quality image with a painting-like effect. In contrast, the Gaussian Kuwahara operator [Fig. 12(d)] produces a worse result with many discontinuities (like, for instance, the ones on the red grapes). Another case is presented in Fig. 13, where a very small image [102×93 pixels, Fig. 13(a)] has been upsampled by a factor of 6, thus obtaining the blurred and low quality image shown in Fig. 13(b). Nevertheless, the proposed operator produces a good quality painting-like picture [Fig. 13(c)].

Finally, Fig. 14 shows the watercolor effect achieved by the proposed operator with large values of σ. Fig. 14(b) shows the output of our operator with $\sigma = 12$ for the test image of Fig. 12(a). Such an effect cannot be achieved by other existing edge-preserving smoothers, like, for instance, the Gaussian Kuwahara filter with the same value of σ [Fig. 12(c)].

B. Influence of the Parameters

In this section, we discuss the influence of the values of the parameters σ, q, and N on the performance of the proposed operator.

The value of σ controls the size of the brush stroke used for the painting: as σ increases, the brush touches become coarser (Fig. 15).

Concerning the number of sectors N, Fig. 16 shows the output of the proposed operator applied to a synthetic noisy

Fig. 12. Example of enlargement: (a) original image (222×150 pixels), (b) image enlarged by a factor 2 and outputs of (c) our and (d) the Gaussian Kuwahara operators with the same value of $\sigma = 3$.
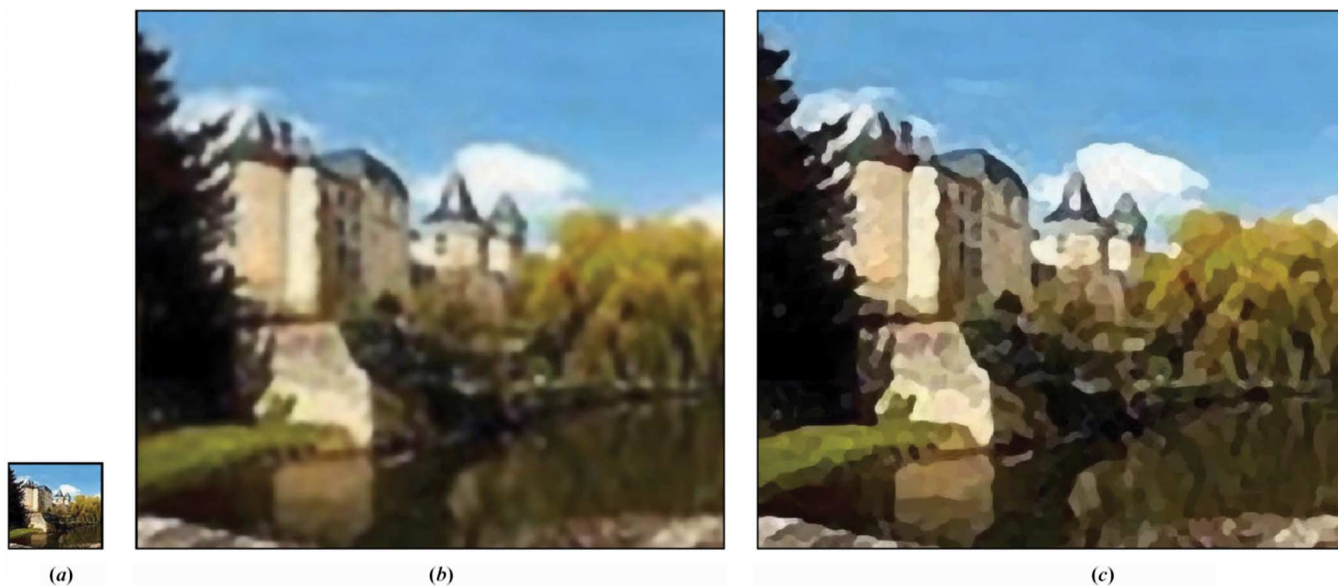
Fig. 13. Another example of enlargement: (a) original image (102×93 pixels), (b) upsampled image by a factor of 6, and (c) the output of the proposed operator. The painting-like effect in the output does not suffer the blur of the enlargement.

image [Fig. 16(a)], for $N = 4, 6, 8$ [Fig. 16(b)–(d)]. We can see that, for these values of N, edge preservation is not significantly influenced by the number of sectors. On the other hand, when higher values of N are used the corners are better preserved,

Fig. 14.   Example of the watercolor effect achieved by our operator with a large value of σ : (a) test image (369 × 568 pixels) and the outputs of (b) our filter and (c) the Gaussian Kuwahara filter for $\sigma = 12$.

TABLE I
VALUES OF THE INPUT PARAMETERS OF THE STUDIED ECPS

Method	Values of the input parameters
Proposed approach	$\sigma = 3$, $N = 8$, $q = 3$
Kuwahara [21]	$a = 5$
Gauss Kuwahara [25]	$\sigma = 3$, four Gaussian windows centered in (±σ, ±σ)
Structural closing [14]	Disk of radius 5 as structuring element
Area open-closing [15]	A_{min} = 50 pixel
Median [13]	5×5 square window
Bilateral [16]	$\sigma = 3$, $\sigma_r = 0.3$. Each color component ranges between 0 and 1

especially the sharper ones, because narrower sectors better fit sharp corners [see Fig. 6(b)]. Noise rejection is not significantly influenced by the value of N. In our experiments, with a large number of images, we found that $N = 8$ gives satisfactory results.

Fig. 17 shows the output of the proposed operator, applied on the test image of Fig. 16(a), for different values of q ($q = 0, 2, 8, \infty$). For $q = 0$, all the coefficients $f_i, i = 1 \ldots N$, are equal [see (10)], so that the proposed operator reduces to a Gaussian smoother. As we see in Fig. 17(a), noise is smoothed, but edges and corners are blurred. As q increases, edges and corner are better preserved [Fig. 17(b)–(d)]. However, beyond a certain value of q, we observe that there is no further improvement in the edge preservation and, on the other hand, noise rejection is worse. This can be easily explained as follows. The case $q \to \infty$ corresponds to the standard minimum variance criterion; thus, noise is averaged only over one sector. Conversely, the case $q = 0$ corresponds to the Gaussian smoother and noise is averaged over an area that is N times larger than in the case

$q \to \infty$. Consequently, for $q = 0$, noise rejection is N times more efficient than for $q \to \infty$.

Fig. 18 plots the noise reduction ratio R as a function of q. R is defined as the ratio between the noise levels after and before the filtering. As we see, R remains rather constant for small values of q, and increases substantially for larger values. We observe that the cases $q = 8$ [Fig. 17(c)] and $q \to \infty$ [Fig. 17(d)] give rise to the same performance in terms of edge and corner preservation, but there are about 4.5 dB of difference in terms of noise rejection in favor of the case $q = 8$. In our experiments with natural images, we found that $q = 8$ is a good compromise between noise and texture reduction and edge preservation.

V. DISCUSSION AND CONCLUSION

Several ECPSs are commonly deployed in image processing applications in order to smooth out noise and texture while preserving or enhancing edges and corners. The ability to sharpen blurred edges, rather than only preserve the already sharp edges in the original image, gives a noticeable contribution to achieving a painting-like effect in the output images. In this paper, we demonstrated that some very common ECPSs, like bilateral [16] or median [13] filtering, are not suitable to accomplish this task, since they are not able to sharpen blurred edges. Moreover, in some cases, the resulting smoothing effect looks more like diffusion or blurring of the texture, rather than a painting-like effect [Fig. 8(e)–(f)]. We showed that structural morphological opening and closing, well known ECPSs, do not give appreciable results either, since the output image presents spots with approximately the same shape and size as the one of the used structuring element. More sophisticated morphological filters based on area open-closing do not suffer
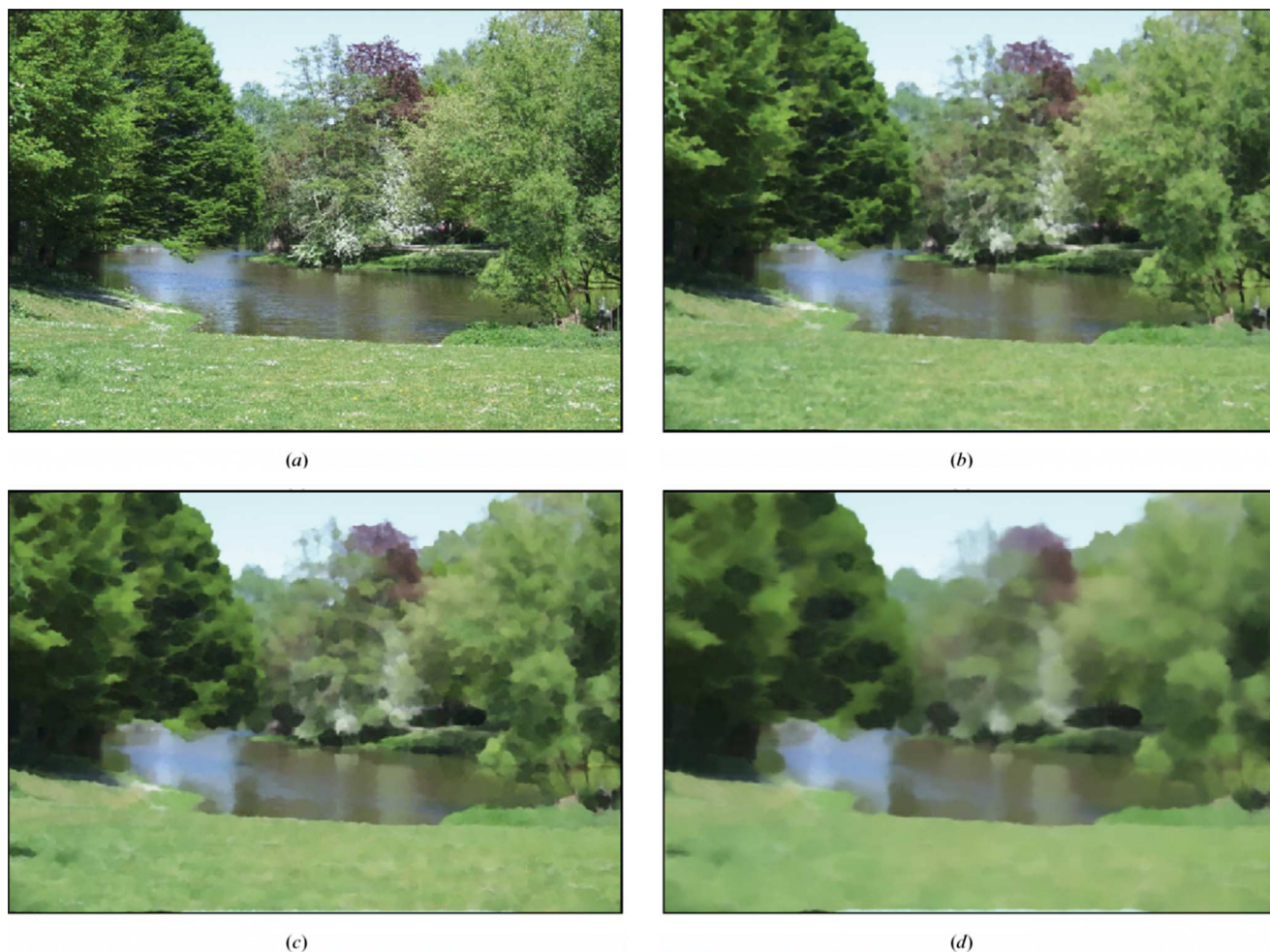
Fig. 15. Influence of σ on the output of the proposed operator. (a) Test image (830 × 623 pixels) and (b), (c), (d) output of the proposed operator for $\sigma = 2, 4, 8$, respectively.
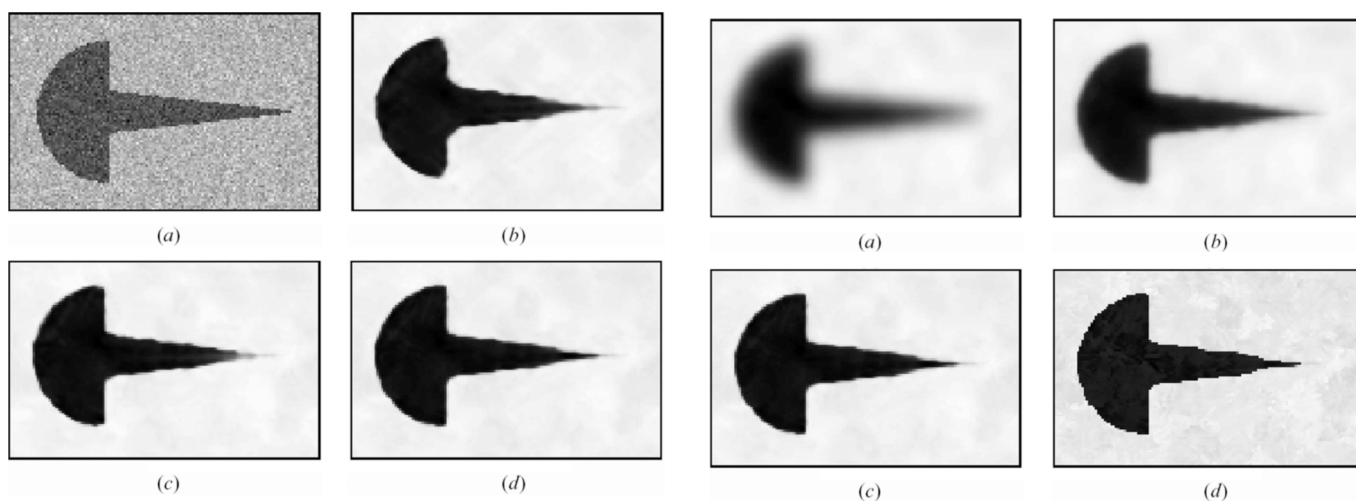

Fig. 16. Influence of the number of sectors N on the output of the proposed operator. (a) Noisy synthetic test image (770 × 340 pixels), and output of the proposed operator for (b) $N = 4$, (c) $N = 6$, and (d) $N = 8$. The values of the other parameters are $\sigma = 4$ and $q = 8$.
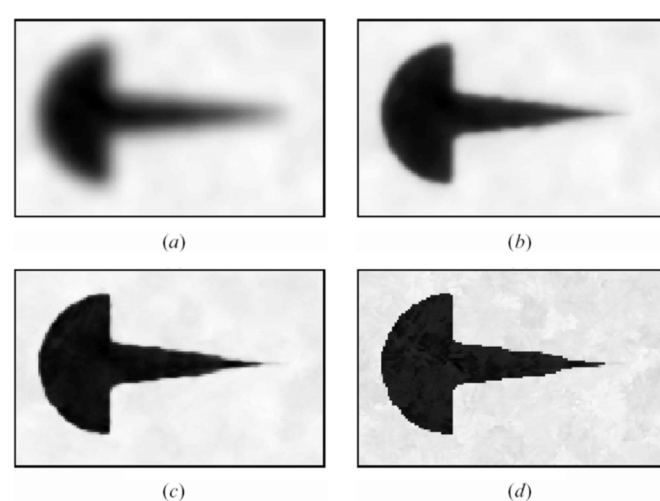
Fig. 17. Output of the proposed operator, applied on the test image of Fig. 15 a, for: (a) $q = 0$, (b) $q = 2$, (c) $q = 8$, and (d) $q \to \infty$. Noise reduction is better visible in the electronic version of the paper.

from the mentioned spot problem and in some cases they are able to produce painting-like images. However, such methods are not robust to blurring and in some cases they do not change appreciably the input image.
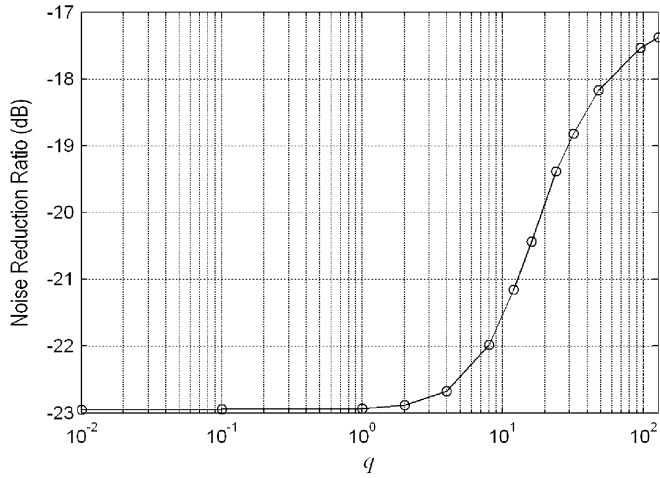
Fig. 18. Noise rejection ratio R of the proposed operator, as a function of q.

A more suitable class of ECPSs for artistic imaging is the value and criterion filter structure [23] that stems from the early work of Kuwahara [21] and its subsequent generalizations. These nonlinear filters are able to smooth out texture while enhancing, not only preserving, edges and corners, and they produce images quite similar to paintings. However, we showed in this paper that such filters are not mathematically well defined operators and give rise to instability in presence of shadowed areas.

In this contribution, we proposed a new EPCS that does not suffer the mentioned limitations. The proposed operator is based on similar principles as the Kuwahara filter but it is mathematically well defined. The chosen form of the weighting functions w_i is particularly suitable for preserving edges and sharp corners and, at the same time, for achieving the same texture rejection level as the Gaussian filtering on edgeless areas.

It is worth pointing out that that our operator, introduced in (11), has some similarity to bilateral filtering [16], defined as

$$\Phi_{\mathrm{bil}}(\mathbf{r}) = \frac{\sum_{\mathbf{x}} I(\mathbf{r}+\mathbf{x}) \cdot w(\mathbf{x}) \cdot d[I(\mathbf{r}), I(\mathbf{r}+\mathbf{x})]}{\sum_{\mathbf{x}} w(\mathbf{x}) \cdot d[I(\mathbf{r}), I(\mathbf{r}+\mathbf{x})]}. \quad (14)$$

In [16], $w(\mathbf{x})$ is the Gaussian kernel (6) and the *range distance* $d(\xi, \eta)$ is proportional to $e^{-(\xi-\eta)^2/2\sigma_r^2}$, where σ_r is an input parameter. Thus, in the weighted average (14), the major contribution is given by those pixels which are spatially closer to point $\mathbf{r}$ and whose gray levels are closer to $I(\mathbf{r})$. The proposed operator has a similar structure: in (11), the weighted sum is over the regions instead over the pixels, and the weighting coefficients s_i^{-q} are determined by the degree of homogeneity of each region, instead of the range distance between each gray level and the central value $I(\mathbf{r})$. The spatial term $w(\mathbf{x})$ does not appear explicitly in (11), but is taken into account by the convolutions (5).

The novelty of bilateral filtering was that the local average (14) is mainly determined by those pixels for which the range distance d is sufficiently high. This fact makes the filter an ECPS. However, its main limitation is that the pixels for which the term $d[I(\mathbf{r}), I(\mathbf{r}+\mathbf{x})]$ is high are spatially unrelated to

each other. The factor $w(\mathbf{x})$ only limits the average (14) on a local neighborhood of $\mathbf{r}$. The proposed approach overcomes this limitation by averaging over regions instead over pixels.

From the computational point of view, the proposed operator is more demanding than the VCFS because the weighting windows $w_i, i = 1 \ldots N$, are not shifted versions of the same window w. Therefore, the number of required convolutions is $2N$ instead of 2.

To summarize, the most significant differences of our approach to previous approaches are: 1) new weighting windows for computing local averages and local standard deviations, 2) a new combination rule which overcomes the ill-posedness of the Kuwahara filter, and 3) adaptive and automatic selection of the of sectors that give a non negligible contribution to the weighted average (11), according to the local pattern around each pixel. Regarding the latter point, all N sectors will be used in a homogeneous texture, while a single sector may be needed at a corner.

The experiments we performed on a wide set of natural images show the effectiveness of the proposed approach in comparison with the above mentioned existing ECPS. We demonstrated that the proposed operator produces a very interesting painting-like effect and that it is robust to image degradation like blurring. We also showed the ability of the proposed operator to produce large high-quality painting-like images starting from small input images.

REFERENCES

[1] J. S. Lee, "Digital image enhancement and noise filtering by use of local statistics," *IEEE Trans. Pattern Anal. Mach. Intell.*, vol. PAMI-2, no. 2, pp. 165–168, Feb. 1980.

[2] D. Wang, A. H. Vagnucci, and C. C. Li, "Gradient inverse smoothing scheme and the evaluation of its performance," *Comput. Graph. Image Process.*, vol. 15, pp. 167–181, 1981.

[3] D. Wang and Q. Wang, "A weighted averaging method for image smoothing," *Proc. ICPR*, pp. 981–983, 1988.

[4] S. M. Smith and J. M. Brady, "SUSAN—A new approach to low level image processing," *Int. J. Comput. Vis.*, vol. 23, no. 1, pp. 45–78, 1997.

[5] B. Smolka and K. Wojciechowski, "Edge preserving image smoothing based on self avoiding random walk," in *Proc. ICPR*, 2000, vol. 3, pp. 668–671.

[6] J. F. Canny, "A computational approach to edge detection," *IEEE Trans. Pattern Anal. Mach. Intell.*, vol. PAMI-8, no. 6, pp. 679–698, Jun. 1986.

[7] P. Saint-Marc, J. S. Chen, and G. Medioni, "Adaptive smoothing: A general tool for early vision," *IEEE Trans. Pattern Anal. Mach. Intell.*, vol. 13, no. 6, pp. 514–529, Jun. 1991.

[8] P. Hall and M. Titterington, "Edge-preserving and peak-preserving smoothing," *Technometrics*, vol. 34, pp. 429–440, 1992.

[9] S. Z. Li, Y. H. Huang, J. S. Fu, and K. L. Chan, "Edge-preserving smoothing by convex minimization," *ACCV*, no. 1, pp. 746–753, 1998.

[10] G. Winkler and V. Liebscher, "Smoothers for discontinuous signals," *J. Nonpar. Statist.*, vol. 14, no. 1–2, pp. 203–222, 2002.

[11] M. Ceccarelli, "Fast edge preserving picture recovery by finite markov random fields," in *Proc. ICIAP*, 2005, pp. 277–286.

[12] M. Hillebrand and C. H. Müller, "On outlier robust corner-preserving methods for reconstructing noisy images," *Ann. Statist.*, vol. 35, no. 1, pp. 132–165, 2007.

[13] W. K. Pratt, *Digital Image Processing.* New York: Wiley, 1978.

[14] H. J. A. M. Heimans, "Connected morphological operators for binary images," *Comp. Vis. Image Understand.*, vol. 73, pp. 99–120, 1999.

[15] A. Meijster and M. H. F. Wilkinson, "A comparison of algorithms for connected set openings and closings," *IEEE Trans. Pattern Anal. Mach. Intell.*, vol. 24, no. 4, pp. 484–494, Apr. 2002.

[16] C. Tomasi and R. Manduchi, "Bilateral filtering for gray and color images," in *Proc. Int. Conf. Comput. Vision*, 1998, pp. 839–846.

[17] D. Comaniciu and P. Meer, "Mean shift analysis and applications," in *Proc. IEEE Int. Conf. Computer Vision*, Kerkyra, Greece, 1999, pp. 1197–1203.

[18] L. I. Rudin, S. O. Stanley, and E. Fatemi, "Nonlinear total variation based noise removal algorithms," *Phys. D*, pp. 250–268, 1992.

[19] P. Perona and J. Malik, "Scale-space and edge detection using anisotropic diffusion," *IEEE Trans. Pattern Anal. Mach. Intell.*, vol. 12, no. 7, pp. 629–639, Jul. 1990.

[20] G. Winkler, K. Hahn, and V. Aurich, "A brief survey of recent edge-preserving smoothers," in *Proc. 5th German-Russian Workshop on Pattern Recognition and Image Understanding*, B. Radig, H. Niemann, Y. Zhuravlev, I. Gourevitch, and I. Laptev, Eds., Herrsching, Germany, Sep. 21-25, 1998, pp. 62–69.

[21] M. Kuwahara, K. Hachimura, S. Ehiu, and M. Kinoshita, "Processing of ri-angiocardiographic images," in *Digital Processing of Biomedical Images*. New York: Plenum, 1976, pp. 187–203.

[22] M. Nagao and T. Matsuyama, "Edge preserving smoothing," *Comput. Graph. Image Process.*, vol. 9, pp. 394–407, 1979.

[23] M. A. Schulze and J. A. Pearce, "A morphology-based filter structure for edge enhancing smoothing," in *Proc. Int. Conf. Image Processing*, 1994, vol. 94, pp. 530–534.

[24] P. Bakker, L. J. van Vliet, and P. W. Verbeek, "Edge preserving orientation adaptive filtering," in *Proc. IEEE Conf. Computer Vision and Pattern Recognition*, Jun. 23–25, 1999, pp. 535–540.

[25] R. van den Boomgaard, "Decomposition of the Kuwahara-Nagao operator in terms of linear smoothing and morphological sharpening," in *Proc. ISMM*, pp. 283–292.

[26] A. V. Oppenheim, R. W. Schafer, and J. R. Buck, *Discrete-Time Signal Processing*, 2nd ed. Englewood Cliffs, NJ: Prentice-Hall, 1999.

Giuseppe Papari was born in Rome, Italy, in 1979. He received the M.S. degree in electrical engineering from the Universita' degli Studi di Roma Tre (University of Rome III) in 2003. He is currently pursuing the Ph.D. degree at the Department of Mathematics and Computing Science, University of Groningen, The Netherlands.

He has published several papers about biologically motivated contour detection, perceptual grouping, and multiresolution analysis, one of which was invited to CODEC 2006. His main research interests are nonlinear filtering, contour detection, image segmentation, multiresolution analysis, clustering, pattern recognition, and morphological analysis.

Dr. Papari received one of the four IBM best student paper awards at the IEEE International Conference on Image Processing in 2006.

Nicolai Petkov received the Dr.Sc.Techn. degree in computer engineering (Informationstechnik) from the Dresden University of Technology, Dresden, Germany.

He is a Professor of computer science and Head of the Research Institute of Mathematics and Computing Science, University of Groningen, The Netherlands. Prior to joining the University of Groningen in 1991, he held research positions at the University of Wuppertal, the University of Erlangen-Nürnberg, the Academy of Sciences in Berlin, and the Dresden University of Technology. He is the author of two monographs and coauthor of another book, holds four patents, and has authored over 100 scientific papers. His current research focuses on computer simulations and understanding the visual system of the brain and using the obtained insights for the development of effective computer vision algorithms. He is also interested in using computers for artistic expression.

Dr. Petkov was awarded an Alexander von Humboldt scholarship of the Federal Republic of Germany in 1989. He is a member of the editorial boards of several journals.

Patrizio Campisi received the Ph.D. degree in electronic engineering from the University of Rome, Roma Tre, Rome, Italy.

He is currently an Associate Professor with the Department of Applied Electronics, University of Rome, Roma Tre. He was a Visiting Researcher at the University of Toronto, Toronto, ON, Canada; at the Beckman Institute, University of Illinois at Urbana-Champaign, Urbana; and at the Ecole Polytechnique de l'Université de Nantes, IRRCyN, France. His research interests have been focused on digital signal and image processing with applications to multimedia. He is co-editor of the book *Blind Image Deconvolution: Theory and Applications* (CRC, 2007). Specifically, he has been working on image deconvolution, image restoration, image analysis, texture coding, texture classification, grayscale, color, and video texture synthesis, watermarking, data hiding, and biometrics.

Dr. Campisi is a corecipient of an IEEE ICIP 2006 best student paper award for the paper titled "Contour detection by multiresolution surround inhibition." He is a Member of the IEEE Communications and Signal Processing Society and the Italian Professional Engineers Association.